Hybrid-graphene gas sensor —Model simulation

A Letters Journal Exploring the Frontiers of Physics

October 2011

EPL, **96** (2011) 10002
doi: 10.1209/0295-5075/96/10002

www.epljournal.org

Hybrid-graphene gas sensor —Model simulation

Shih-Jye Sun[1(a)] and Chung-Yi Lin[2]

[1] *Department of Applied Physics, National University of Kaohsiung - Kaohsiung 811, Taiwan, R.O.C.*
[2] *Department of Physics, National Chung Hsing University - Taichung 402, Taiwan, R.O.C.*

received 18 May 2011; accepted in final form 9 August 2011
published online 13 September 2011

PACS 07.07.Df – Sensors (chemical, optical, electrical, movement, gas, etc.); remote sensing
PACS 73.22.Pr – Electronic structure of graphene

Abstract – We propose and theoretically investigate the physical properties of an alternative design of graphene gas sensor, composed of a nanoscaled gas-inert conducting wire between two graphene leads. The sensing mechanism is based on the conduction variation in the nanoscaled conducting wire as a result of a density-of-states change in the graphene leads via the orbital hybridization established between the graphene leads and the absorbed gas molecules. We use the coherent potential approximation to treat the disordered system resulting from the random gas molecule absorption and apply the Keldysh non-equilibrium Green's function method to calculate the transport properties. Compared with the conventional gas sensors that use graphene as the conducting wire, the one proposed here is superior, especially for charge-donor gases.

Gas sensors are widely used in monitoring miscellaneous systems especially the atmosphere [1]. Although various types of gas sensors are designed according to different physical mechanisms such as resistive [2], dielectric [3], and optical [4] properties of the working substance, nevertheless, accuracy, fast response, and sensitivity are the universal requirements for the instrument. Among all the function modes, the resistive-type gas sensors is the most simple in structure and commonly used for detecting the atmosphere. Up to now, no single gas sensor is capable of sensing all kinds of gas molecules. This is because the functional response to the interaction between the sensor host and the adsorbed gas molecules may not be strong enough to produce detectable signals, let alone in some cases there is no reaction at all. For this reason, both choosing proper materials and designing ensemble structures with vigorous effects are important for producing versatile gas sensors. Primarily, the detecting key in the resistive-type of gas sensors depends on its conducting variation as gas molecule is adsorbed by the host. Obviously, it takes large adsorbing-surface to produce significant response signal for detection. Porous and nano-rod or -wire structures [5–8] are suitable candidates for the device because they satisfy the requirement in the surface issue.

Experimental results have shown that carbon nanotube (CNT) has the capability to result conductivity variations from adsorbing various types of gas molecules [9–12]. Gas molecules absorption on CNT occurs by means of the orbital hybridization of the dangling π bonds on CNT and the gas molecule orbitals [13]. The gas adsorption process can be resulted from either physical or chemical reaction determined on the bonding form. Graphene, a single-layer carbon sheet composed of similar honeycomb lattices, is similar to CNT, which also has the dangling π bonds perpendicular to the carbon sheet with the capability of gas adsorption [14–17]. In addition, graphene is a gapless material with good conductivity.

Considering the interplay of the gas adsorption process and the conductivity, we propose a hybrid-graphene-structure gas sensor that is similar in structure to the conventional graphene gas sensors but with a total different concept. The schematic structure of the gas sensor is represented in fig. 1, which comprises two large graphene leads that are connected by a nanoscaled gas-inert conducting molecular wire with each graphene lead lying on the top of a metal pad. In most graphene-made sensors, the grahene is used to play the role of the conducting wire and the sensing mechanism relys upon its electrical conduction variations as it adsorbs the gas molecules. Nevertheless, in the conventional graphene-made sensors, the current passing through the graphene wire inevitably makes the graphene become dynamical, and the conduction can also be affected by some defects in the lead contacts connecting to the graphene wire. On the contrary, in our proposed sensor, since graphene

(a) E-mail: sjs@nuk.edu.tw

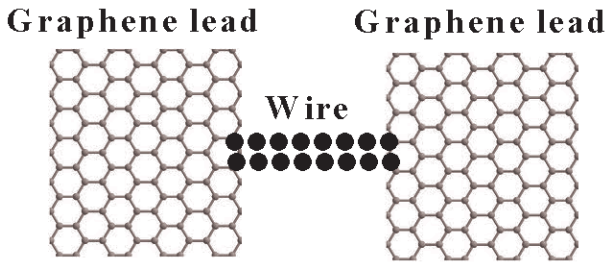

Fig. 1: The schematic structure of the hybrid-graphene gas sensor that is composed of two large graphene leads, each sitting on the top of a metal pad (which is not shown in this figure), with a gas-inert conducting molecular wire connecting the leads.

is only used as the leads, it remains in the static state as the applied bias is applied. When the graphene lead adsorbs the gas molecules, the change of its density of states (DOS) consequently results in a current variation in the molecular wire. Definitely, the difference between the proposed gas sensor and the conventional ones is that the detecting key of the former lies in the leads, but not in the conducting wire. An orbital hybridization model is constructed to analyze our idea for the hybrid-graphene gas sensor. Through this model we calculate the conduction variation of the device as the graphene adsorbs gas molecules. Two energy parameters, the orbital hybridization interaction and the bound-states orbital energy level of the gas relative to the free orbital energy level of graphene, are utilized to simulate the adsorption of the individual gas molecule by the graphene lead.

Except for the saturate adsorption, the original periodic system of graphene becomes disordered as the gas molecules are adsorbed. The Hamiltonian of the disordered system is given by

$$H = \sum_{k,\sigma} \epsilon_k c^+_{k,\sigma} c_{k,\sigma} + V \sum_{i\in A,\sigma} \xi_i (c^+_{i,\sigma} d_{i,\sigma} + \text{h.c}) + E_d \sum_{i\in A,\sigma} \xi_i d^+_{i,\sigma} d_{i,\sigma} + \epsilon_p \sum_{i\in A,\sigma} (1-\xi_i) c^+_{i,\sigma} c_{i,\sigma}. \quad (1)$$

The first term of eq. (1) represents the kinetic energy of the graphene, which is obtained by the tight-binding approximation and contains two split bands,

$$\epsilon_k = \frac{e_p \pm t \times w_k}{1 \pm ss \times w_k}, \quad (2)$$

where t is the hopping integral, ss is the overlapping function between π orbits, and $w_k = 1 + 4\cos(\frac{\sqrt{3}k_x}{2})\cos(\frac{k_y}{2}) + 4\cos^2(\frac{k_y}{2})$ [13] is the energy dispersion of the graphene; the second term describes the orbital hybridization between the graphene and the gas molecules, in which ξ_i is 1 or 0 depending on whether the carbon site, i, is attached with a gas molecule or not; E_d in the third term represents the orbital energy of the carbon atom in the graphene attached with a gas molecule, while ϵ_p in the last term represents the orbital energy of the carbon atom that is free from gas adsorption.

Coherent potential approximation (CPA) is a well-developed method for studying the disordered systems [18,19]. The description of CPA aims to replace the originally disordered Hamiltonian by an effective periodic Hamiltonian. The effective Hamiltonian $\overline{H}$ is obtained by modulating the original Hamiltonian by a self-energy matrix.

$$\overline{H} = \sum_{k,\sigma} \epsilon_k c^+_{k,\sigma} c_{k,\sigma} + \sum_{i,\sigma} \begin{pmatrix} c^+_{i,\sigma} & d^+_{i,\sigma} \end{pmatrix} \begin{pmatrix} S_{cc} & S_{cd} \\ S_{dc} & S_{dd} \end{pmatrix} \begin{pmatrix} c_{i,\sigma} \\ d_{i,\sigma} \end{pmatrix}, \quad (3)$$

where S_{cc}, S_{cd}, S_{dc} and S_{dd} are the elements of the self-energy matrix and the real-valued $S_{cd} = S_{dc}$ assures the Hermiticity of the Hamiltonian.

The difference between the disordered and the effective Hamiltonian contains effective scattering potentials V_A and V_B, in which subscript A corresponds to the sites where gas molecules can be adsorbed, while subscript B denotes the sites where there is no gas molecules adsorbed:

$$H - \overline{H} = \sum_i V_i \quad (4)$$

$$= \sum_{i\in A} \xi_i V_A + \sum_{i\in A} (1-\xi_i) V_B, \quad (5)$$

where V_A and V_B and are given by

$$V_A = \begin{pmatrix} -S_{cc} & V - S_{cd} \\ V - S_{dc} & E_d - S_{dd} \end{pmatrix}, \quad V_B = \begin{pmatrix} \epsilon_p - S_{cc} & -S_{cd} \\ -S_{dc} & -S_{dd} \end{pmatrix}. \quad (6)$$

Consequently, we obtain the T matrices from the above potentials for gas adsorbing and non-adsorbing sites, respectively, which are

$$T_{A(B)} = \frac{V_{A(B)}}{1 - F(\omega) V_{A(B)}}, \quad (7)$$

where the function

$$F(\omega) = \frac{1}{N} \sum_k (\omega - \overline{H})^{-1} = \frac{1}{N} \sum_k \overline{G}(\omega, k).$$

Based on the CPA, the elements of the self-energy matrix in eq. (3) are deduced from the self-consistent equation,

$$x T_A + (1-x) T_B = 0, \quad (8)$$

where $x = \langle \xi_i \rangle$ is the coverage ratio of the adsorption.

The conducting channel in the gas sensor is a gas-inert conducting molecular wire, for example, a gold wire. If the length of the wire is of nanoscale, we can calculate the current as a function of applied bias by means of

the Keldysh current formula [20]. Furthermore, if only the interaction with the graphene leads is included, the Keldysh formula has a compact form as

$$I = \frac{e}{h}\int \mathrm{d}\epsilon[f_L(\epsilon+v_a) - f_R(\epsilon)]T_r\{G^a(\epsilon)\Gamma^R(\epsilon)G^r(\epsilon)\Gamma^L(\epsilon)\}, \tag{9}$$

where $f_{L(R)}$ is the Fermi-Dirac distribution function for the left (right) lead; $\Gamma^{L(R)}(\epsilon) = 2\pi V_{L(R)}^2 D_{L(R)}(\epsilon)$ is the broadening function resulting from the left (right) lead-wire interaction, and $D_{L(R)}(\epsilon)$ is the DOS of the left (right) graphene lead; function of $G^{r(a)}(\epsilon)$ is the retarded (advanced) Green's function and these Green's functions can be derived from the Hamiltonian of the molecular wire. In addition, the chemical potential in the Fermi-Dirac distributions, $f_{L,R}$, is determined by the measure of charge transfer, Δn, between the graphene and the adsorbed gas molecules that determined via the orbital hybridization coupling strength V. $\Delta n = r \times x$ represents the average amount of exchanged charge per carbon atom in the graphene that is the product of the absorbing coverage ratio, x, and the charge exchange ratio, r. The charge exchange ratio, r, can be either positive or negative depending on whether graphene acts as a charge acceptor or a charge donor, respectively.

The simplest form of the Hamiltonian of the gas-inert conducting molecular wire is given by

$$H = t_0\sum_i d_i^+ d_{i+1} + E_0 d_i^+ d_i + \sum_k V_L(c_k^+ d_1 + \text{h.c.}) + \sum_k V_R(c_k^+ d_N + \text{h.c.}), \tag{10}$$

where t_0 is the hopping integral and E_0 is the orbital energy in the molecular wire under the single-orbit approximation. The last two terms of eq. (10) represent the lead-wire interactions under the assumption that the nanoscaled molecular wire interacts with the leads with coupling constants only through the contacting atoms at the two ends. Although this assumption is very ideal, we evaluate it will not lose the contact property qualitatively, especially for the graphene lead with a large bandwidth. The atoms at the ends of the wire are labelled with subscripts 1 and N and interact with the left and the right graphene lead via coupling constants V_L and V_R, respectively. The lead-wire interactions at the two ends of the conducting wire gives rise to the lead-wire self-energies for the contacting molecules that are given by

$$\Sigma_{\alpha\in L,R}(\epsilon) = \sum_{k,\eta\to 0}\frac{V_\alpha^2}{\epsilon - \epsilon_k + i\eta}. \tag{11}$$

If the bandwidth of the graphene is much larger than that of the conducting wire then the self-energy can be approximated by $\Sigma_{\alpha\in L,R}(\epsilon) = -i\pi V_\alpha^2 D_\alpha(\epsilon)$ where $D_\alpha(\epsilon)$ is the density of states of the grapheme leads.

Some parameters of this study are set as follows: $t = -3$ for the hopping integral of graphene, $t_0 = -1$ for the hopping integral of the conducting wire, $N = 50$ for the molecule numbers of the conducting wire, $ss = 0.13$ for the π orbital function overlap, $\epsilon_p = 0$ for the orbital energy level of the graphene, and $V_{L,R} = 1.0$ for the lead-wire couplings. In addition, all energies are in the units of eV and the temperature is set to 300 K.

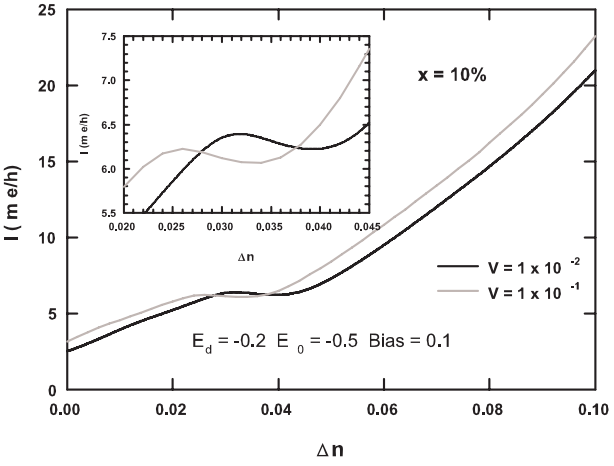

Fig. 2: The current I as a function of the transferred charge Δn at the adsorption coverage ratio $x = 10\%$ for different hybridization coupling strength V. Inset zooms in the limited region for the current deviation.

The sensing mechanism of our graphene gas sensor is manifested by the response of current variation in a gas-inert conducting wire that is caused by the change of DOS in the graphene leads as they adsorb gas molecules. Physically, it is the charge transfer between the graphene and the adsorbed gas molecules that modifies the chemical potential and dominates the transport of the conducting wire. Figure 2 exhibits the current in the conducting wire as a function of transferred charge, Δn, at the adsorption coverage ratio $x = 10\%$ for various hybridization coupling strength V. With Δn is defined as a net charge transferred to a graphene molecule, it can be seen that except for a small deviated region the current for charge acceptor graphene (*i.e.* positive Δn), increases monotonically with Δn. The inset exhibits the zoom-in of the deviated region. These current profiles indirectly reflect the effect of chemical potential to the DOS of the graphene with hybridized orbits. The chemical potential is originally set to zero for the gas-free graphene, but chemical potential becomes negative owing to the orbital hybridization that localizes the carriers and increases the DOS at the same time. Furthermore, the orbital hybridization also splits a single band into two and produces a DOS valley between the two split bands. Since the chemical potential, which is elevated by an increase of charge transfer, will pass through the DOS valley and give rise to a current decrease as shown in the inset of fig. 2.

The fact that the amount of charge transfer Δn determines whether the current is increased or decreased as a result of gas molecule adsorption is confirmed by the current variations shown in fig. 3. It can be seen in

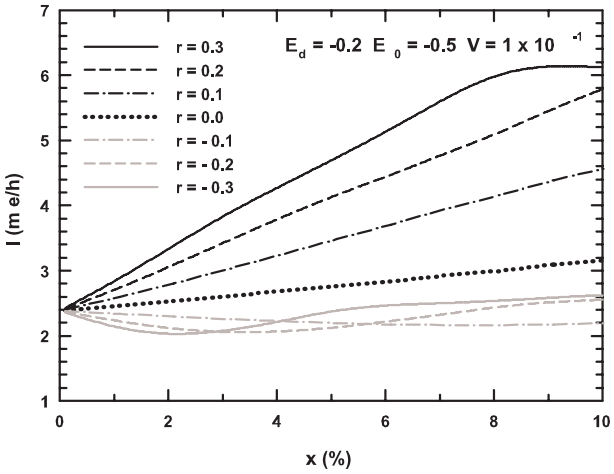

Fig. 3: The current I in the conducting wire as a function of the adsorption coverage ratio x with transferred charge $\Delta n = r \times x$ assumed. Positive and negative charge transfer ratio, r, corresponds to charge acceptor and charge donor graphene, respectively.

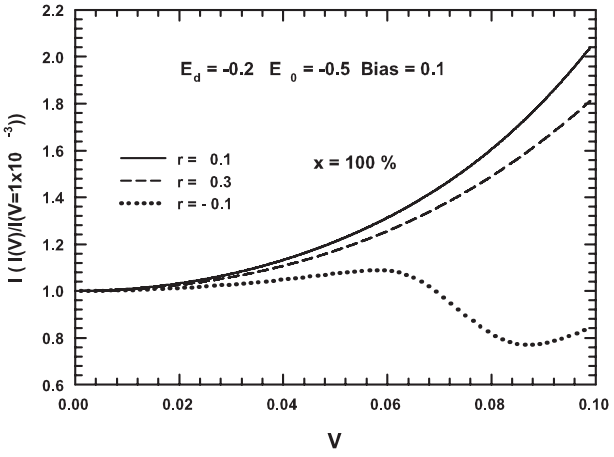

Fig. 4: The normalized current as a function of the orbital hybridization strength V for the saturate, $x = 100\%$, charge acceptor and charge donor graphenes at bias $= 0.1$. The bound energy level $E_d = -0.2$, and the orbital energy $E_0 = -0.5$.

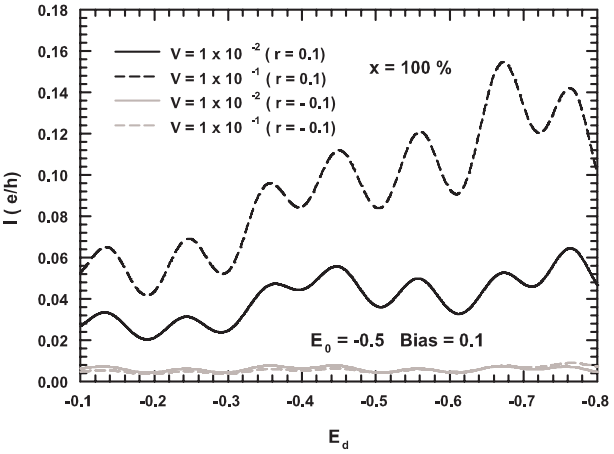

Fig. 5: The currents as a function of E_d for saturate charge acceptor and charge donor graphenes for various orbital hybridization strength V. The bias is 0.1 volt, bound level $E_0 = -0.5$ and the charge transfer ratios for charge acceptor and charge donor graphene are $r = 0.1$ and $r = -0.1$, respectively.

fig. 3 that the currents associated with charge acceptor graphenes increase as more gas molecules are absorbed while the device with charge donor graphenes are rather insensitive to gas adsorption. In detail, in the case of charge donor graphene, for the charge transfer ratio up to $r = -0.3$, there is a global decreasing currents for small coverage ratio x, but after some critical value of r, the currents rise up again at larger values of x. Compared to the conventional design of graphene gas sensor, namely, using the graphene as the conducting channel, that the decrease or increase of current depends on the properties of the adsorbed gas molecules [16,17], our hybrid-graphene gas sensor is able to provide more property information for the adsorbed gas molecules, *i.e.* charge donor gases always increase the current, and yet charge acceptor gases behave rather oppositely.

In our model, two energy parameters, V and E_d, are used to describe the effect of an individual gas molecule. V refers to the orbital hybridization coupling strength between the graphene and adsorbed gas molecules, which strongly affects charge transfer and certainly affects the conduction of the device, and E_d represents the orbital energy of the carbon atom in the graphene attached with a gas molecule. Figure 4 exhibits the normalized current as a function of V for charge acceptor and charge donor graphenes at the saturate adsorption, *i.e.*, $x = 100\%$. For the case of charge acceptor graphene the current varies parabolically as a function of V. However, for the case of charge donor graphene the current increases slightly at small V, and yet decreases as V gets large. This result also implies that charge-donor graphene is able to make the current decrease for various kinds of gas molecules.

As a gas molecule is adsorbed to a carbon atom, the carbon energy level of the π orbital changes from ϵ_p to a bound state, E_d, under the condition of stable adsorption $E_d < \epsilon_p$. Figure 5 shows the currents as a function of E_d for saturated charge acceptor and charge donor graphenes for various V. The current amplitude for the case of charge acceptor graphene increases with V, but that for the case of charge donor graphene does not show significant differences between various V, which means that the gas sensor is superior in detecting charge donor gases than charge acceptor gases. An important feature of fig. 5 is that the currents oscillate with a regular interval of E_d, which is 0.1 at the parameters we set up. Such a regularity found in the current as a function of E_d is a result that as E_d increases the chemical potential crosses the energy levels of the conducting wire. In other words, this regular energy interval of E_d is the difference of energy states of the wire.

In summary, we propose a microscopic theory for analyzing the physical properties of gas molecules adsorbed on the graphene leads and subsequently develop a new design of hybrid-graphene gas sensor. The main structure of gas sensor is composed of two graphene leads that are connected by a gas-inert conducting molecular wire and its sensing ability is derived from electrical current variation in the conducting wire. The underlying mechanism is that there are charge transfers taking place as the gas molecules are adsorbed on the graphene leads that changes the density of states of the graphene and consequently causes the current variation in the conducting wire. The gas sensor proposed is superior compared to the conventional design, which uses graphene for the conducting wire, specially for the charge donor gas detection.

* * *

This work was supported by the National Science Council in Taiwan through Grant Nos. NSC-98-2112-M-390-001-MY3 (S-JS) and NSC-98-2112-M-005-004-MY3 (C-YL), and by the National Chung Hsing University. The hospitality of the National Center for Theoretical Sciences, Taiwan, where the work was initiated, is gratefully acknowledged.

REFERENCES

[1] Pearton S. J., Ren F., Wang Y. L., Chu B. H., Chen K. H., Chang C. Y., Lim W., Lin J. and Norton D. P., *Prog. Mater. Sci.*, **55** (2010) 1.
[2] Kong J., Franklin N. R., Chou C., Chaplin M. G., Peng S., Cho K. and Dai H., *Science*, **287** (2000) 622.
[3] Chopra S., McGuire K., Gothard N. and Rao A. M., *Appl. Phys. Lett.*, **83** (2003) 2280.
[4] Penza M., Cassano G., Aversa P. and Antolini F., *Appl. Phys. Lett.*, **85** (2004) 2379.
[5] Liu J., Luo T., Meng F., Qian K., Wan Y. and Liu J., *J. Phys. Chem. C*, **114** (2010) 4887.
[6] Firooz A. A., Hyodo T., Mahjoub A. R., Khodadadi A. A. and Shimizu Y., *Sens. Actuators B*, **147** (2010) 554.
[7] Yu J., Ippolito S. J., Wlodarski W., Strano M. and Zadeh K. K., *Nanotechnology*, **21** (2010) 265502.
[8] Lupan O., Ursaki V. V., Chai G., Chow L., Emelchenko G. A., Tiginyanu I. M., Gruzintsev A. N. and Redkin A. N., *Sens. Actuators B*, **144** (2010) 56.
[9] Zhang T., Mubeen S., Myung N. V. and Deshusses M. A., *Nanotechnology*, **19** (2008) 332001.
[10] Valentini L., Armentano I., Kenny J. M., Cantalini C., Lozzi L. and Santucci S., *Appl. Phys. Lett.*, **82** (2003) 961.
[11] Collins P. G., Bradley K., Ishigami M. and Zettl A., *Science*, **287** (2000) 1801.
[12] Novak J. P., Snow E. S., Houser E. J., Park D., Stepnowski J. L. and McGill R. A., *Appl. Phys. Lett.*, **83** (2003) 4026.
[13] Saito R., Dresselhaus G. and Dresselhaus M. S., *Physical Properties of Carbon Nanotubes* (Imperial College, London) 2003.
[14] Schedin F., Geim A. K., Morozov S. V., Hill E. W., Blake P., Katsnelson M. I. and Novoselov K. S., *Nat. Mater.*, **6** (2007) 652.
[15] Romero H. E., Joshi P., Gupta A. K., Gutierrez H. R., Cole M. W., Tadigadapa S. A. and Eklund P. C., *Nanotechnology*, **20** (2009) 245501.
[16] Wehling T. O., Novoselov K. S., Morozov S. V., Vdovin E. E., Katsnelson M. I., Geim A. K. and Lichtenstein A. I., *Nano Lett.*, **8** (2008) 173.
[17] Fowler J. D., Allen M. J., Tung V. C., Yang Y., Kaner R. B. and Weiller B. H., *ACS Nano*, **3** (2009) 301.
[18] Soven P., *Phys. Rev.*, **156** (1967) 809.
[19] Taylor D. W., *Phys. Rev.*, **156** (1967) 1017.
[20] Haug H. and Jauho A.-P., *Quantum Kinetics in Transport and Optics of Semiconductors* (Springer-Verlag) 1998.